

BEAM MONOCHROMATIZATION CONCEPTS FOR POWDER DIFFRACTION

Detlef Beckers, Milen Gateshki, Detlev J. Götz
Malvern Panalytical B.V., Almelo, The Netherlands

ABSTRACT

Many applications of X-ray diffraction, like structural crystallography, deconvolution of complex patterns for phase identification and quantification of multiple-phase mixtures, benefit from monochromatic X-rays. Traditional incident monochromators include, for example, Johansson monochromators, 4-crystal-monochromators or the so-called hybrid monochromators - i.e. combinations of a parabolic graded multilayer with a channel cut crystal. Their advantages lie in the high degree of monochromatization and beam collimation, which result typically in XRD measurements with improved peak to peak resolution, peak shape and a significant improvement of the peak-background ratio. However, significant drawbacks typically include a strong reduction of intensity and limited experimental flexibility due to geometrical restrictions. Here, we discuss alternative concepts for beam monochromatization and compare their advantages and disadvantages with traditional incident monochromating optics.

FLEXIBLE $K\alpha_1$ SYSTEM

A higher geometrical flexibility in a $K\alpha_1$ -setup can be realized by the separation of the monochromatization functionality from the beam collimation. This can be achieved by using e.g. a Johansson monochromator for the $K\alpha_1$ monochromatization together with a graded multilayer (X-ray mirror) to “shape” the beam and determine the beam geometry at the sample: an elliptical mirror can be used to achieve a focusing transmission geometry, a flat mirror can be used in Bragg-Brentano reflection geometry (Figure 1) or a parabolic mirror is used to create a parallel beam. In such a set-up the multilayer also typically further improves the $K\alpha_2$ -suppression of the Johansson monochromator.

With the possibility to position the tube either before the Johansson monochromator or before the mirror (the Johansson monochromator is then not used anymore) such a system offers additional flexibility to switch between $K\alpha_1$ radiation (with monochromator) for higher resolution or $K\alpha_{1,2}$ radiation (if only the mirror is used) for higher intensity.

Figure 2 shows the application of the described $K\alpha_1$ transmission set-up on a $C_4H_8O_4$ sample (glycolaldehyde dimer, provided by Institute Ruđer Bošković, Zagreb) with Cu radiation. The sample was indexed with the TREOR (Werner *et al.*, 1985) and DICVOL04 (Boultif and Louër, 1991) algorithm as implemented in HighScore (Degen *et al.*, 2014). The intensities have been extracted by Pawley fit, and the structure was solved by direct methods (Mohaček-Grošev *et al.*). The broad hump observed in the background between approximately 15° and $25^\circ 2\theta$ is due to scattering originating from the capillary and was modelled with a polynomial function in the analysis.

This document was presented at the Denver X-ray Conference (DXC) on Applications of X-ray Analysis.

Sponsored by the International Centre for Diffraction Data (ICDD).

This document is provided by ICDD in cooperation with the authors and presenters of the DXC for the express purpose of educating the scientific community.

All copyrights for the document are retained by ICDD.

Usage is restricted for the purposes of education and scientific research.

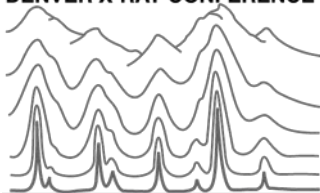
DXC Website

– www.dxcicdd.com

ICDD Website

- www.icdd.com

DENVER X-RAY CONFERENCE®



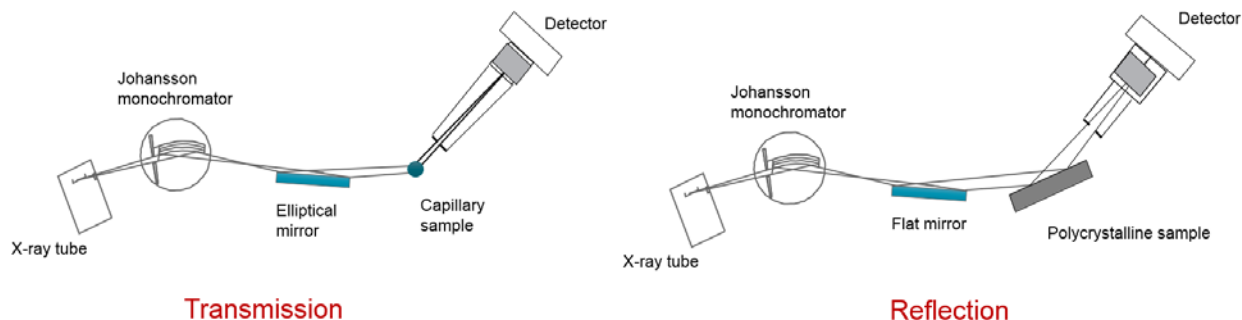


Figure 1: Schematic drawings of a $K\alpha_1$ -setup with graded multilayer (X-ray mirror). The X-ray mirror determines the beam collimation. Typically, an elliptical mirror is used to create a convergent X-ray beam optimized for transmission geometry. A flat graded mirror creates a divergent beam for Bragg-Brentano geometry. It is also possible to use a parabolic mirror (not shown) that creates a parallel beam. For each type of collimation different anti-scatter shielding can be used in front of the detector.

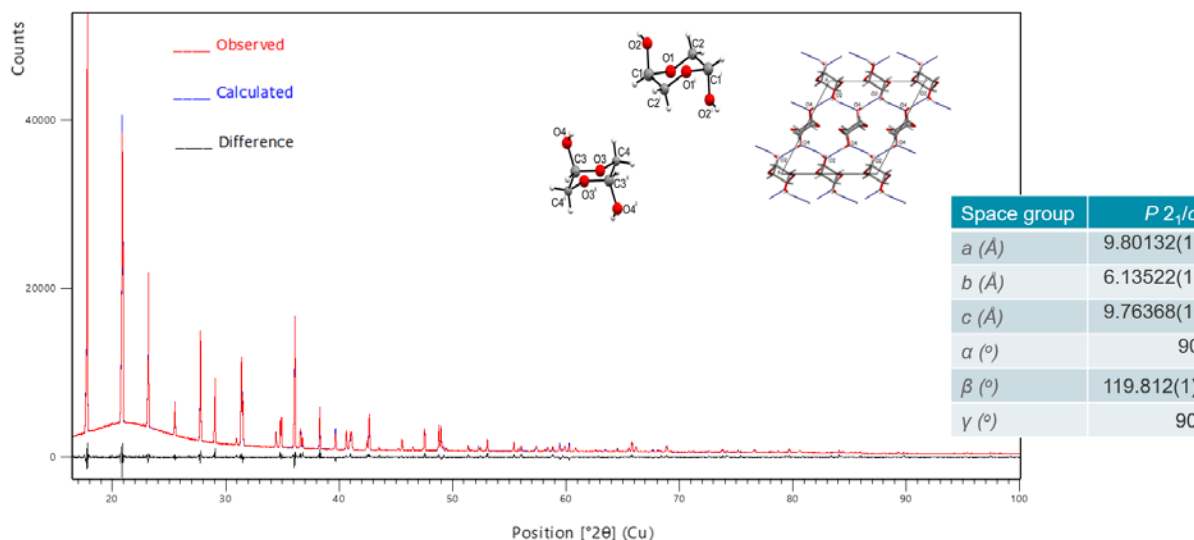


Figure 2: Data collected in $Cu K\alpha_1$ transmission set-up from $C_4H_8O_4$. The table shows the determined space group and unit cell geometry from the refined structure.

MONOCHROMATIZATION WITH BETA RADIATION

Traditionally monochromators are using the $K\alpha_1$ line of the spectrum since this is the most intense characteristic line. In some cases, however, other characteristic lines for beam monochromatization are useful. Table 1 shows the relative intensities and the photon energies of the main characteristic lines of typical anode materials.

Radiation	K_{edge} [keV (I_{rel})]	$K\beta_2$ [keV (I_{rel})]	$K\beta_1$ [keV (I_{rel})]	$K\beta_3$ [keV (I_{rel})]	$K\alpha_1$ [keV (I_{rel})]	$K\alpha_2$ [keV (I_{rel})]
Co	7.712		7.649 (20%)		6.930 (100%)	6.915 (51%)
Cu	8.993	8.978 (0.1%) 0.5% of $\beta_{1,3}$	8.905 / 8.903 (20%)		8.048 (100%)	8.028 (51%)
Mo	20.002	19.960 (3%)	19.608 (15%)	19.590 (8%)	17.479 (100%)	17.374 (52%)
Ag	25.531	25.463 (4%)	24.943 (16%)	24.912 (9%)	22.163 (100%)	21.991 (53%)

Table 1: Relative intensities (to the $K\alpha_1$) and photon energies of the main characteristic lines of typical anode materials.

For anode materials up to $Z=29$ (Cu), the $K\beta$ lines can be considered to have single energy and be a good candidate for beam monochromatization. A detector with sufficiently good energy resolution can separate $K\alpha$ - from $K\beta$ -radiation directly, without a monochromator in the beam path. This would be most beneficial for measurements using the Bragg-Brentano para-focusing geometry.

Alternatively, the $K\beta$ line can be selected with a multilayer mirror. The mirror can then be used at the same time for beam collimation. This configuration, however, has the limitation that the $K\alpha$ -radiation is usually not suppressed sufficiently unless two multilayers are employed, but this would make the set-up more complex. A possible solution is to use a combination of a graded $K\beta$ multilayer optic and a detector with good energy resolution that can suppress the remaining $K\alpha$ -radiation from the mirror sufficiently. With such a set-up a flexible geometry (either reflection / transmission or parallel beam geometry) can be realized, in which a $K\beta$ -mirror can be used to collimate the beam (beam shaper) and the monochromatization of the beam will be achieved from the multilayer in combination with the detector. This set-up can easily be implemented on diffraction systems with only a small intensity loss of $K\beta$ -radiation. In transmission geometry $K\beta$ -radiation often has the additional advantage of higher transmission through the sample compared to $K\alpha_1$ radiation from a Johansson monochromator. Figure 3 shows a comparison of a transmission $K\alpha$ and $K\beta$ and a reflection $K\alpha_1$ measurement on a $CrF_3 \cdot 3H_2O$ sample (intensities scaled and $K\beta$ radiation pattern converted to $K\alpha_1$ wavelength). The data shows that the $K\beta$ radiation pattern has similar quality as the $K\alpha_1$ pattern and shows only a slightly increased peak asymmetry.

The crystal structure of $CrF_3 \cdot 3H_2O$ has been reported by Herbstein et al. The reported crystal structure is extremely disordered giving rise to an unrealistic structural model. Consequently, we attempted to re-investigate the crystal structure of this material using monochromatic radiation. A peak splitting of the reflection (101) (R-3m setting) is clearly visible around $21.7^\circ 2\theta$ in the $CuK\alpha_1$ data. This peak splitting is confirmed by synchrotron data collected at Alba. This is suggesting that the correct crystal structure of $CrF_3 \cdot 3H_2O$ is of lower symmetry than previously reported and is currently being investigated but this is beyond the scope of the current contribution.

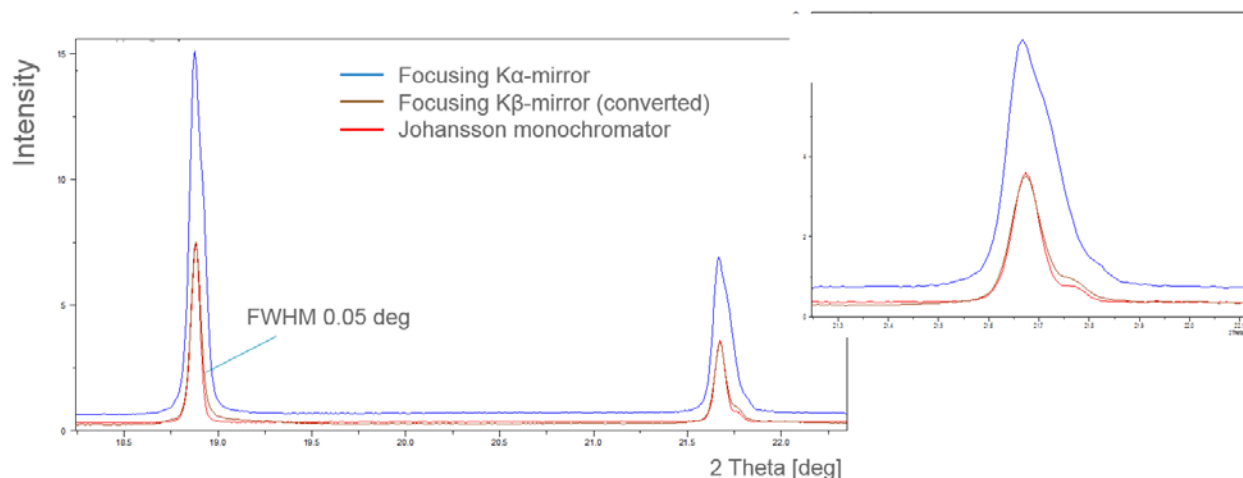


Figure 3: (a) Comparison of a transmission $K\alpha$ and $K\beta$ and a reflection $K\alpha_1$ measurement on a $\text{CrF}_3 \cdot 3\text{H}_2\text{O}$ sample (intensities are scaled for better comparison of profile shapes and the $K\beta$ radiation pattern is converted to $K\alpha_1$ wavelength). In the measurements with monochromatic radiation the peak splitting of the reflection at around $21.7^\circ 2\theta$ becomes clearly visible. The data shows (insert (b)) that the $K\beta$ radiation pattern has similar quality as the $K\alpha_1$ pattern and has only a slightly higher peak asymmetry.

The same approach of utilizing $K\beta$ -radiation can also be used for X-rays produced with other types of anode materials. For example, the application of Ag $K\beta$ radiation is demonstrated in the next example. Figure 4 shows Ag $K\alpha$ and Ag $K\beta$ transmission measurements on an iPhone 4s battery (discharged state). This battery has a thickness of $\sim 4\text{mm}$. Measurements have been performed with graded elliptical X-ray mirrors (see schematic in Figure 5). As already mentioned above, in the Ag $K\beta$ measurement the Ag $K\alpha$ component is not completely removed by the multilayer mirror. In this case however, with increasing the thickness of the sample, the so-called beam hardening effect in the sample is further monochromatizing the diffracted beam (Ag $K\alpha$ is more strongly absorbed than Ag $K\beta$ radiation). This effect is further illustrated in Figure 6.

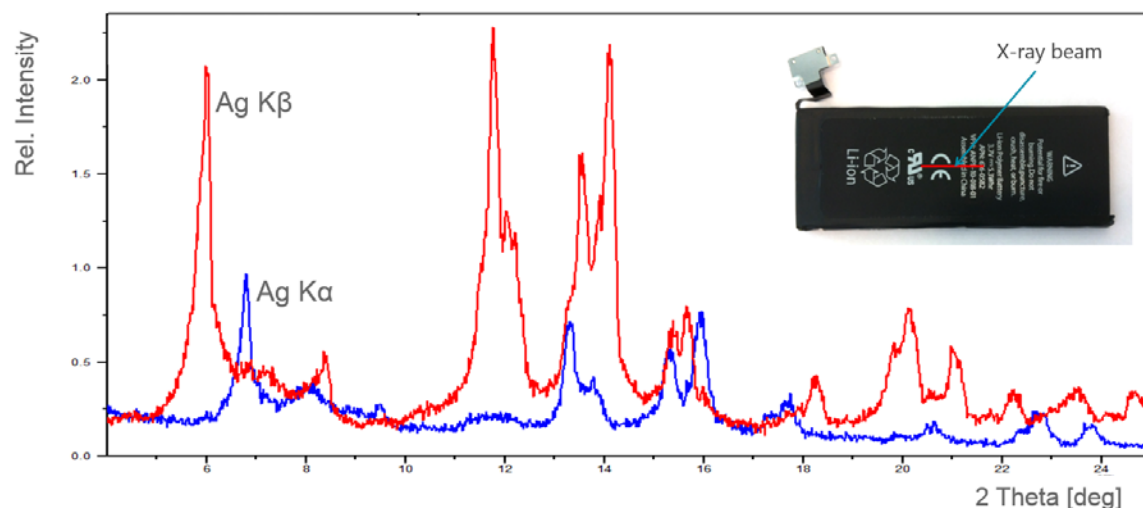


Figure 4: Ag $K\alpha$ and Ag $K\beta$ transmission measurements on an iPhone 4s battery (discharged state).

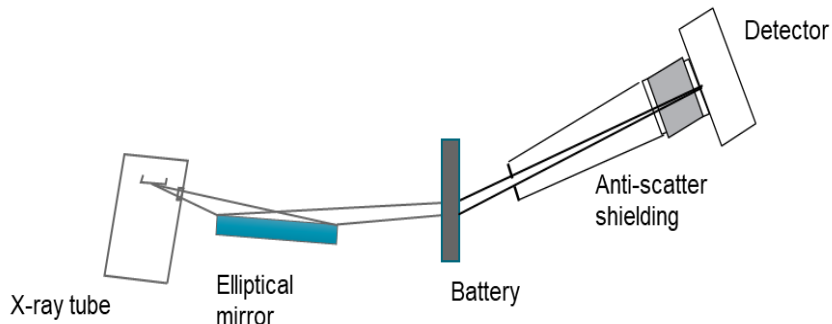


Figure 5: Schematic drawing of a setup with graded focusing multilayer X-ray mirror to measure a battery in transmission geometry. The mirror can either be optimized for Ag $K\alpha$ or for Ag $K\beta$ radiation.

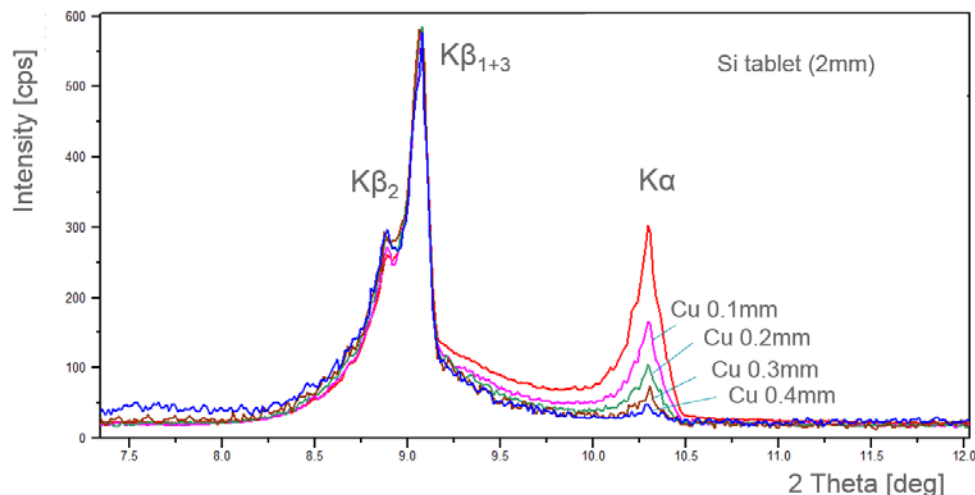


Figure 6: Beam hardening effect demonstrated with measurements of a sample, which is a combination of a 2 mm thick Si tablet and Cu foils of different thicknesses. Patterns are scaled to the maximum of the Ag $K\beta_{1+3}$ line. The contribution of the $K\alpha$ line in the diffraction pattern decreases as the absorption of the sample increases.

Measurements of a 5mm thick battery can be simulated by adding an additional absorber to the battery discussed above. In this case, the Ag $K\alpha$ line is almost completely absorbed whereas the Ag $K\beta$ line still produces meaningful diffraction data (Figure 7). As shown in Table 1, the Ag $K\beta$ line is effectively a triplet, but due to the geometrical aberrations in transmission measurements on (very) thick samples, which broaden the diffraction peaks, the diffraction lines appear effectively as a single asymmetric peak. In cases like this, where the broadening of the diffraction peaks due to sample effects is significant compared to the peak separation between $K\beta_{1+3}$ and $K\beta_2$, the pattern could be treated as being produced by monochromatic radiation.

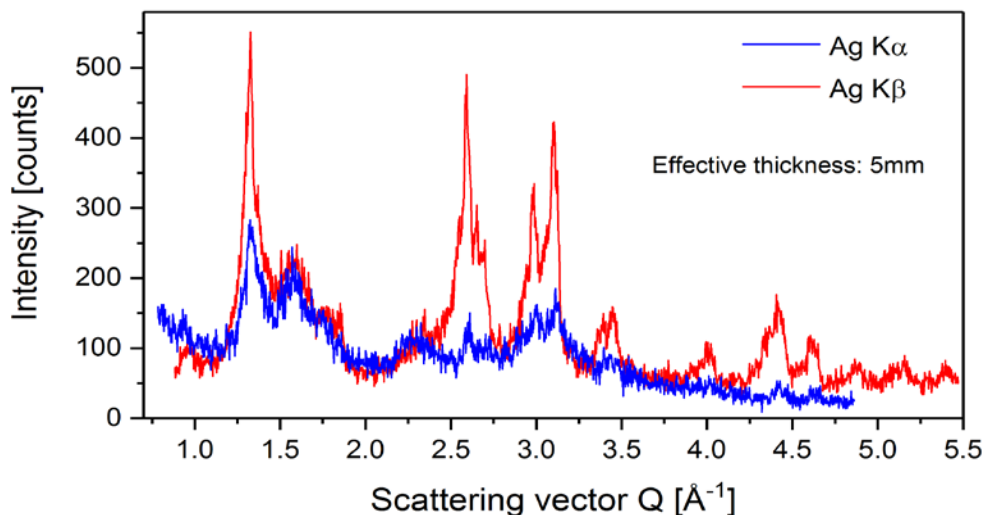


Figure 7: Measurements of a battery with effective thickness of ~5 mm using Ag $K\alpha$ and Ag $K\beta$ radiation. The patterns are plotted against the scattering vector Q . The measurement with Ag $K\beta$ radiation shows well defined diffraction peaks. On the other hand, the diffraction signal measured with the Ag $K\alpha$ radiation is nearly lost in the background, especially at higher diffraction angles.

FILTER BASED MONOCHROMATIZATION

In X-ray diffractometers filters are typically used to remove $K\beta$ radiation, wherein the material of the filter must have an absorption edge between the $K\alpha$ and the $K\beta$ lines of the selected anode material. Consequently, the $K\beta$ radiation is stronger absorbed than the $K\alpha$ radiation. Using this principle, monochromatization of the X-ray beam can also be achieved with the use of filters by considering the absorption edges and characteristic lines of different elements with absorption edges between the $K\alpha_1$ and the $K\alpha_2$ line of other elements (see Table 2).

Target element	Energy $K\alpha_2$ [keV]	Energy $K\alpha_1$ [keV]	Filter element	K absorption edge [keV]
47 Ag	21.9903	22.1629	44 Ru	22.119
57 La	33.0341	33.4418	53 I	33.166
58 Ce	34.2789	34.7197	54 Xe	34.590
59 Pr	35.5502	36.0263	55 Cs	35.987
79 Au	66.9895	68.8037	73 Ta	67.403
82 Pb	72.8042	74.9694	76 Os	73.856
83 Bi	74.8148	77.1079	77 Ir	76.101
90 Th	89.953	90.534	83 Bi	93.350

Table 2: Overview of possible target elements and related filter material having an absorption edge between the $K\alpha_1$ and the $K\alpha_2$ line of the target element (Hosoya, 1968).

From the materials presented in Table 2 the combination of Ag as a target material and Ru as a filter is the most promising for practical applications, suppressing the Ag $K\alpha_1$ radiation much stronger than the Ag $K\alpha_2$. Due to this property, Ru can be used for beam monochromatization in a diffractometer using a tube with Ag anode (Figure 8). Although the Ru filter absorbs the Ag $K\alpha_2$ radiation (7.75 times), the Ag $K\alpha_1$ line is almost completely removed ($< 0.02\%$), and the Ag $K\beta$ line is reduced to less than 0.5% of the Ag $K\alpha_2$ radiation. The high peak asymmetry of the Ag $K\alpha_2$ line and a high-angle tail on the right side of the peak are caused by the filter (absorption edge).

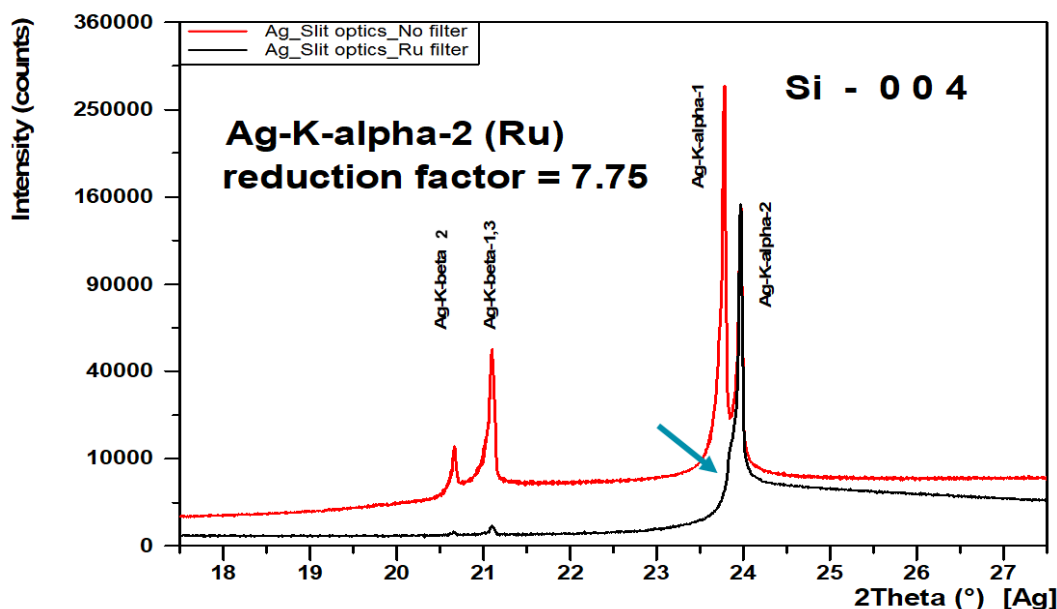


Figure 8: Bragg-Brentano measurements on a Si single crystal using Ag radiation without and with monochromating Ru filter. The filtered pattern was scaled by a factor 7.75 to match the intensity of the unfiltered $K\alpha_2$ line. The arrow marks the absorption edge of the Ru filter.

There are several possibilities to reduce the high-angle tails and the peak asymmetry of the Ag $K\alpha_2$ line, for example by using a detector with good energy resolution which would allow the removal of most of the high-angle tail and the reduction of the background intensity as well. Other options are to apply multi-layer optics or graphite monochromators. Figure 8 shows measurements of LaB_6 with the combination of a Ru filter and a graded parabolic multilayer (Ag mirror). The Ru filter monochromatizes the beam and then the Ag mirror determines the geometrical properties of the beam (divergent, parallel, or convergent) and reduces the background and the high-angle tails. In such a set-up, unfiltered Ag $K\alpha_{1+2}$ radiation can be used for high intensity measurements and filtered Ag radiation (i.e., Ag $K\alpha_2$) can be used for high resolution work with the simple addition of a Ru filter. In Figure 9 the Ru filter reduced the Ag $K\alpha_2$ diffraction peaks by 5 times compared to those unfiltered. Also, the Ag $K\alpha_1$ peaks were reduced to less than 0.5% of the corresponding Ag $K\alpha_2$ peaks; the Ag $K\beta$ peaks were not detected. This performance is comparable to dedicated incident single crystal monochromators for Ag $K\alpha_1$ radiation and is expected to produce data with similar quality. The high-angle tail can

be reduced also by using a balanced filter (Berman and Ergun, 1970). In the case of Ag radiation however, the balanced filter includes Tc-containing material, which due to its radioactivity is unlikely to be applied in most standard laboratory diffractometers.

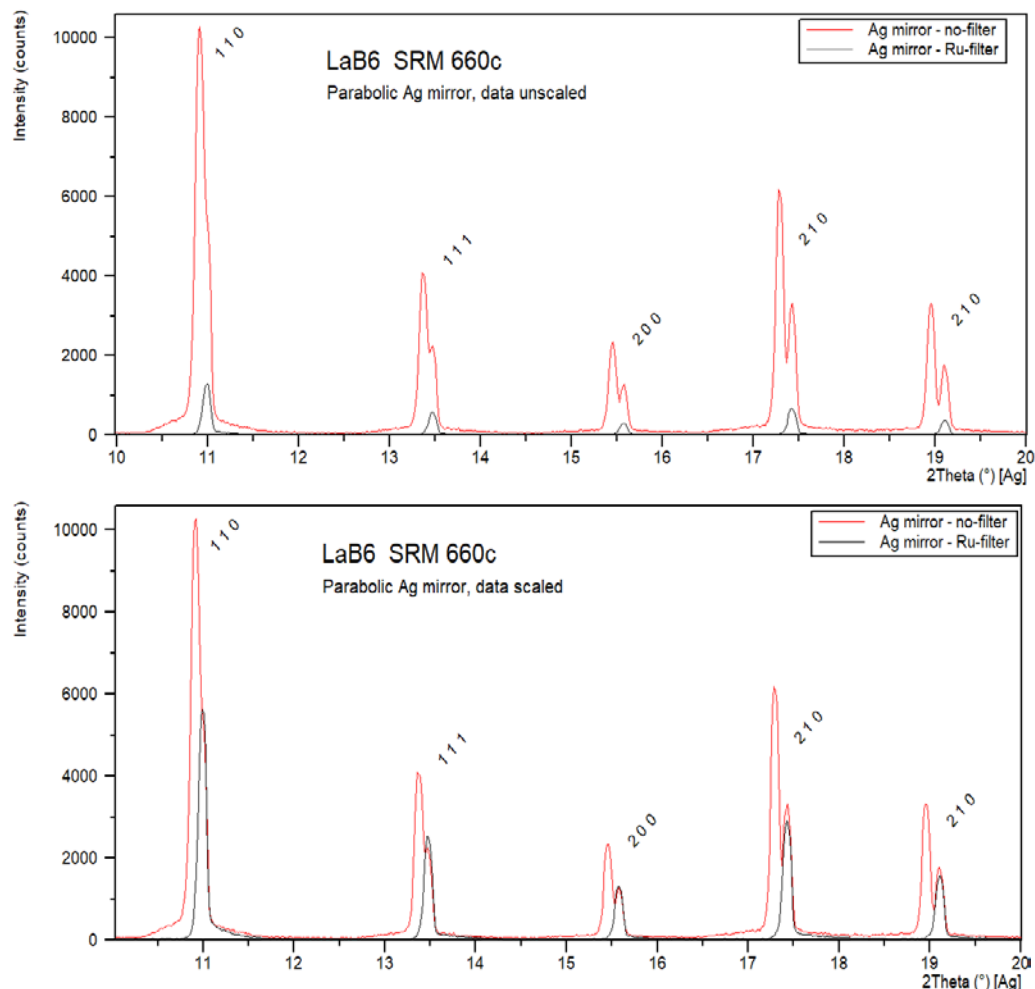


Figure 9: Measurements on LaB₆ with a parabolic Ag mirror. In red the measurement without Ru filter and in black the measurement with Ru filter. The upper graph displays the unscaled patterns; in the lower graph the data is scaled to the same Ag K α_2 intensity. The Ru filter reduced the Ag K α_2 line approximately 5 times. Ag K α_1 was reduced to less than 0.5% of Ag K α_2 and Ag K β was not detected.

SUMMARY

Beam monochromatization methods using a combination of detectors, mirrors, filters, etc. provide alternatives to traditional incident K α_1 monochromators and, in some cases, offer increased flexibility in the X-ray diffractometers. Graded multilayer optics can be used to define the geometrical properties of the beam and to suppress some of the undesired spectral features of the X-ray beam. Additional monochromators, detector settings or filters can be used to improve the monochromatization of the beam created by the mirror.

ACKNOWLEDGEMENT

We thank Prof. Kerstin Forsberg for the synthesis of the $\text{CrF}_3 \cdot 3\text{H}_2\text{O}$ sample and Dr. François Fauth for the beamtime allocation on the BL04-MSPD beamline at the Alba synchrotron.

REFERENCES

- Berman M., Ergun S. (1970). “Balanced Filters for K-alpha X-rays”, *Rev. Sc. Instr.* **41**, 870-873.
- Boultif A. and Louër D. (1991). “Indexing of powder diffraction patterns for low-symmetry lattices by the successive dichotomy method”, *J. Appl. Cryst.*, **24**, 987 – 993.
- Degen T., Sadki M., Bron E., König U., Nénert G. (2014). *Powder Diffr.* **29**, 13–18.
- Herbstein F. H., Kapon M., Reisner G.M. (1985). *Zeitschrift für Kristallographie - Crystalline Materials*, **171**, 209–224.
- S. Hosoya S. (1968). “The K-alpha2 radiation monochromated by a new filter and its topographical and other applications”, *Jap. J. Appl. Phys.* **7**, 1 – 6.
- Mohaček-Grošev V., Prugovečki B., and Prugovečki S. (in preparation) “Second crystal structure of glycolaldehyde dimer does not reveal equatorial OH groups“.
- Werner P.E., Erikson L. and Westdahl M. (1985). “TREOR, a semi-exhaustive trial-and-error powder indexing program for all symmetries”, *J. Appl. Cryst.*, **18**, 367 – 370.